



Enzymatic conjugation of a bioactive peptide into an injectable hyaluronic acid–tyramine hydrogel system to promote the formation of functional vasculature



Li-Shan Wang, Fan Lee, Jaehong Lim, Chan Du, Andrew C.A. Wan, Su Seong Lee, Motoichi Kurisawa*

Institute of Bioengineering and Nanotechnology, 31 Biopolis Way, The Nanos, Singapore 138669, Singapore

ARTICLE INFO

Article history:

Received 22 October 2013
Received in revised form 30 January 2014
Accepted 11 February 2014
Available online 21 February 2014

Keywords:

Hydrogel
Vascularization
RGD
Hyaluronic acid
Functionalization

ABSTRACT

In this study, one-step enzyme-mediated preparation of a multi-functional injectable hyaluronic-acid-based hydrogel system is reported. Hydrogel was formed through the in situ coupling of phenol moieties by horseradish peroxidase (HRP) and hydrogen peroxide (H_2O_2), and bioactive peptides were simultaneously conjugated into the hydrogel during the gel formation process. The preparation of this multi-functional hydrogel was made possible by synthesizing peptides containing phenols which could couple with the phenol moieties of hyaluronic-acid–tyramine (HA–Tyr) during the HRP-mediated crosslinking reaction. Preliminary studies demonstrated that two phenol moieties per molecule resulted in a consistently high degree of conjugation into the HA–Tyr hydrogel network, unlike the one modified with one phenol moiety per molecule. Therefore, an Arg–Gly–Asp (RGD) peptide bearing two phenol moieties (phenol₂–poly(ethylene glycol)–RGD) was designed for conjugation to endow the HA–Tyr hydrogel with adhesion signals and enhance its bioactivities. Human umbilical vein endothelial cells (HUVECs) cultured on or within the RGD-modified hydrogels showed significantly different adhesion behavior, from non-adherence on the HA–Tyr hydrogel to strong adhesion on hydrogels modified with phenol₂–poly(ethylene glycol)–RGD. This altered cell adhesion behavior led to improved cell proliferation, migration and formation of capillary-like network in the hydrogel in vitro. More importantly, when HUVECs and human fibroblasts (HFF1) were encapsulated together in the RGD-modified HA–Tyr hydrogel, functional vasculature was observed inside the cell-laden gel after 2 weeks in the subcutaneous tissue. Taken together, the in situ conjugation of phenol₂–poly(ethylene glycol)–RGD into HA–Tyr hydrogel system, coupled with the ease of incorporating cells, offers a simple and effective means to introduce biological signals for preparation of multi-functional injectable hydrogels for tissue engineering application.

© 2014 Acta Materialia Inc. Published by Elsevier Ltd. All rights reserved.

1. Introduction

Hydrogels are widely used as scaffolds for tissue engineering [1]. The aqueous three-dimensional (3-D) environment within a hydrogel is not only suitable for the encapsulation of cells, but is also capable of presenting biological signals in the form of bioactive peptides grafted or incorporated into the gel network. Presentation of bioactive peptides aims to recapitulate the extracellular matrix (ECM) of the tissue to be regenerated and/or stimulate the encapsulated cells with specific biological signals. There are two main approaches to introduce bioactive peptides into a hydrogel network.

The first is a step-wise approach in which peptide-conjugated synthetic/natural polymers are first synthesized and subsequently crosslinked to form a hydrogel [2–7]. The second is a one-step preparation approach in which peptides containing reactive groups are conjugated into the hydrogel network during the crosslinking reaction in situ [8–11]. For example, the enzymatic activity of Factor XIIIa was employed to covalently incorporate a variety of exogenous oligopeptide mimetics or pairs of them at controllable concentrations within the fibrin network during coagulation [10]. This in situ conjugation provided a simple and effective approach to endow fibrin with adhesion and morphogenetic signals that are not naturally present within the material. At the same time, an extensive alteration to the inherent properties of the materials was avoided during the modification process, unlike its step-wise counterpart where the modification is directly made to the polymers.

* Corresponding author. Tel.: +65 6824 7139; fax: +65 6478 9083.

E-mail address: mkurisawa@ibn.a-star.edu.sg (M. Kurisawa).

Hyaluronic acid (HA), a non-sulfated glycosaminoglycan found in the ECM, has been widely used to form hydrogels for biomedical applications. HA is most abundant during early embryogenesis and plays critical roles in regulating the angiogenic process and wound healing [12,13]. Although naturally derived, it can be commercially produced using microbial fermentation. Therefore it is a promising material for making tissue engineering scaffolds due to its low immunogenicity and biodegradability. However, HA is known to resist cell adhesion, limiting the use of HA-based gels for some tissue engineering applications. Several methods have been developed to enhance the cell-adhesive property of hydrogels, including the incorporation of Arg–Gly–Asp (RGD) peptide [4,9,14] into the gel matrices or ECM components such as fibronectin [15] collagen [16] and fibrin [17]. The presence of RGD, a well-known cell adhesion ligand found in fibronectin, is found not only to promote integrin-mediated cell adhesion, but also to enhance the activity of endothelial cells [18–21]. As insufficient vascularization remains a major challenge to overcome in order to form thicker and more complex tissues, there have been numerous attempts to promote the formation of the vascular network in the engineered constructs for effective tissue engineering by incorporating or grating ECM proteins, ECM-derived peptides or signaling protein including the RGD peptide [2,22–30].

Previously we described an injectable hyaluronic acid–tyramine (HA–Tyr) hydrogel system formed by enzyme-mediated crosslinking of tyramine moieties using horseradish peroxidase (HRP) and hydrogen peroxide (H_2O_2). The HRP-mediated crosslinking reaction has become an attractive method to form hydrogels in situ due to its substrate specificity, efficiency and lack of involvement of toxic crosslinkers [17,31–39]. The HRP-mediated coupling of phenol moieties could further be utilized for the in situ conjugation of bioactive peptides into the hydrogel network. Indeed, Park et al. recently demonstrated the conjugation of an endothelial cell binding peptide, Ser–Val–Val–Tyr–Gly–Leu–Arg, into a gelatin–PEG–tyramine (GPT) hydrogel by HRP-mediated crosslinking [8]. This endothelial cell binding peptide terminates with a tyrosine residue which readily forms C–C or C–O bonds with the tyramine moieties of GPT during the crosslinking reaction. The modified cell-free GPT hydrogel was able to influence the activity of endothelial cells in surrounding tissues and enhance angiogenic activity and cell migration to the construct.

In this paper, a detailed study was first performed to examine the coupling efficiency of phenol-containing RGD peptides into the HA–Tyr hydrogel network using two model compounds, one bearing a single phenol moiety while the other bearing two phenol moieties. Having confirmed that a molecule containing two phenol moieties had a more consistent coupling efficiency and resulted in hydrogels with superior rheological properties, we proceeded to design an RGD peptide bearing two phenol moieties per molecule (phenol₂–PEG–RGD; PEG = poly(ethylene glycol)). The phenol₂–PEG–RGD was readily conjugated into HA–Tyr hydrogels during gel formation process by the HRP-mediated crosslinking reaction. The RGD-modified hydrogels (HA–Tyr–RGD) were then characterized in terms of rheology, water uptake and cell adhesion, proliferation and migration. Furthermore, human umbilical vein endothelial cells (HUVECs) and human fibroblasts (HFF1) were mixed together with phenol₂–PEG–RGD and HA–Tyr conjugates to form a cell-laden HA–Tyr–RGD hydrogel for the purpose of promoting a capillary-like network in the hydrogel. The cell-laden HA–Tyr–RGD hydrogels were found not only to promote a capillary-like network in the hydrogel in vitro, but also to result in functional vasculature 2 weeks after the gel injection into the subcutaneous tissue. We believe that this one-step preparation of the injectable HA–Tyr hydrogel system with additional peptide motifs via HRP-mediated crosslinking provides a new platform to customize the gel with multiple bioactive motifs tailored to the tissue of interest.

2. Materials and methods

2.1. Materials

HA (90 kDa) was kindly donated by JNC Corp. (Tokyo, Japan). Type I collagenase ($246 \text{ units mg}^{-1}$), hyaluronidase from bovine testes and Triton X-100 were purchased from Sigma–Aldrich. Hydrogen peroxide was from Lancaster and HRP, 100 units mg^{-1} was from Wako Pure Chemical Industries. Dulbecco's modified Eagle medium (DMEM), fetal bovine serum (FBS), penicillin–streptomycin, Quant-iT™ PicoGreen® dsDNA Reagent and Kits and CellTracker Green CMFDA were provided by Life Technologies (Singapore). An actin cytoskeleton and focal adhesion staining kit containing vinculin monoclonal antibody, tetramethylrhodamine isothiocyanate (TRITC)-conjugated phalloidin and 4',6-diamidino-2-phenylindole (DAPI) and human nuclei antibody (MAB 1281) were provided by Millipore (Singapore). Mouse monoclonal anti-CD31 antibody (ab9498) was obtained from Abcam. An anti-mouse HRP-DAB cell and tissue staining cell was purchased from R&D systems (USA). A Pierce™ BCA protein assay kit was obtained from Thermo Scientific (Singapore).

2.2. Synthesis and characterization of phenol₂–PEG–RGD

The phenol₂–PEG–RGD was synthesized by using an automatic synthesizer Titan 357 (AAPTEC). 50 mg of ChemMatrix® resins (0.48 mmol g^{-1}) was swelled in 1 ml of *N*-methylpyrrolidone (NMP) for 5 min in a reaction vessel (RV). With the liquid drained, 1 ml of 20% piperidine in NMP (v/v) was added and the RV was vortexed for 2 min. The liquid was drained and 1 ml of fresh solution (20% piperidine in NMP, v/v) was added. The RV was vortexed for another 10 min. The resulting beads were thoroughly washed with NMP (1 ml \times 2), methanol (1 ml \times 2) and dichloromethane (DCM, 1 ml \times 2), successively. With the resulting resins swelled with NMP for 15 min, Fmoc-D(OtBu)-OH (2.5 equiv, 0.2 M solution in NMP) was added to the RV, as well as *N,N,N',N'*-tetramethyl-*O*-(benzotriazol-1-yl)uronium tetrafluoroborate (TBTU, 2.5 equiv, 0.2 M solution in NMP) and *N,N*-diisopropylethylamine (DIEA, 5.0 equiv, 0.5 M in NMP). The resulting mixture was vortexed for 45 min. With the liquid drained, the resulting beads were thoroughly washed with NMP (1 ml \times 3). The coupling step was repeated until the desired structure attained on beads, i.e., HPA–K(Mtt)–PEG2(13 atm)–R(Pbf)–G–D(OtBu). Then, selective deprotection of the 4-methyltrityl (Mtt) group was performed by reaction with 2 ml of trifluoroacetic acid/triisopropylsilane/DCM (TFA/TIS/DCM, 3/3/94, v/v/v) for 2 min, 5 min and 30 min successively, using a fresh aliquot each time. Finally, another group of 3-(4-hydroxyphenyl) propionic acid (HPA) was coupled to the exposed amine group at the residue of K. The resins were washed with NMP (1 ml \times 3) and transferred in a 4 ml reactor equipped with a filter, using DCM (2 ml \times 3). After the resins were dried under reduced pressure for 2 h, the peptide was cleaved in a cleavage cocktail of TFA–water–TIS (1.5 ml, 94/3/3, v/v/v) for 2 h on a 180° shaker, while all the acid-labile protective groups in the residues were also detached. The solution was collected and concentrated in a continuous flow of nitrogen and the crude peptides were precipitated in diethylether. The resulting white solid was then purified to >98% in purity by preparative high-performance liquid chromatography (HPLC; Gilson) on a C18 reversed phase preparative column (Kromasil®, 21.2 mm \times 250 mm) using water and acetonitrile with 0.1% TFA as the mobile phase. The absorbance of phenol₂–PEG–RGD (0.1 mM) was measured at 276 nm using an ultraviolet–visible (UV–vis) spectrophotometer (U-2810, Hitachi, Japan) and was compared to that of HPA (0.1 mM).

2.3. Formation and rheological properties of HA–Tyr–RGD hydrogels

The synthesis of HA–Tyr conjugate was reported in detail previously [32,37]. The degree of substitution (the number of tyramine molecules per 100 repeating units of HA) was calculated from proton nuclear magnetic resonance measurements and was found to be 5. To form the hydrogels, lyophilized HA–Tyr was dissolved in phosphate buffered saline (PBS) at a concentration of 1 wt.%. In the case of HA–Tyr–RGD hydrogels, phenol₂–PEG–RGD was mixed with HA–Tyr solution to give the final concentrations of 0.1 and 0.2 mM. Then, 1.5 µl of HRP was added to 250 µl of the mixture solution to give a final concentration of 0.15 units ml⁻¹. Crosslinking was initiated by adding 1.5 µl of H₂O₂ solution to give final concentrations of 0.43 mM. The mixture was vortexed vigorously before it was applied to the bottom plate in a HAAKE Rheoscope 1 rheometer (Karlsruhe, Germany). The upper cone was then lowered to a measurement gap of 0.03 mm and a layer of silicon oil was carefully applied around the cone to prevent solvent evaporation during the experiment. The measurements were taken at 37 °C in the dynamic oscillatory mode with a constant deformation of 1% and frequency of 1 Hz. The measurement parameters were determined to be within the linear viscoelastic region in preliminary experiments.

2.4. Conjugation efficiency of phenol₂–PEG–RGD and water uptake of the resulting hydrogels

Conjugation efficiency of phenol₂–PEG–RGD in the hydrogel was estimated by the determination of unconjugated phenol₂–PEG–RGD leached out from the hydrogel after overnight soaking. The amount of unconjugated phenol₂–PEG–RGD was determined by bicinchoninic acid (BCA) assay. In the swelling ratio study, hydrogels were allowed to set for 6 h before being incubated with PBS solution. They were removed from PBS solution after 24 h and blotted to remove excess solution and immediately weighed. Water uptake was calculated from the equation $W = (M_s - M_d) / M_d$, where M_s is the weight of the hydrogel in the swollen state and M_d is the dry weight of the hydrogel obtained by lyophilization.

2.5. Cell culture

HUVECs and endothelial growth medium (EGM-2) BulletKit were purchased from Lonza Bioscience Singapore. HFF1 cells were obtained from ATCC (USA). HUVECs were maintained in EGM-2 BulletKit while fibroblasts were maintained in DMEM supplemented with 15% FBS and 1% penicillin/streptomycin. Both cell types were cultured in T75 tissue culture flasks and incubated at 37 °C in a 5% CO₂ atmosphere. Change of media was carried out every 2–3 days and the cells were subcultured at 80% confluency. Fibroblasts with a passages number lower than 8 and HUVECs between passage 6 and 8 were used in this study.

2.6. In vitro two-dimensional (2-D) culture on hydrogel

For 2-D cell culture on the surfaces of HA–Tyr and HA–Tyr–RGD hydrogels, the hydrogels were prepared on a 24-well plate using the same protocol as described above. The final concentration of H₂O₂ was 0.43 mM. For the hydrogels involved in the following in vitro and in vivo studies, HA–Tyr, phenol₂–PEG–RGD, HRP and H₂O₂ solutions were sterilized by filtering using syringe filters with a pore size of 0.2 µm. The hydrogels were allowed to set for 4 h after the initiation of crosslinking by HRP and H₂O₂. 250 µl of HUVECs in complete medium at a cell density of 1×10^5 cells ml⁻¹ was seeded onto the surfaces of the hydrogels. The HA–Tyr hydrogel without RGD modification was prepared to serve as a

comparison. The culture medium was changed every 2–3 days. At each time interval, the cells attached to the hydrogel surfaces were harvested by incubation overnight at 37 °C with 200 µl of hyaluronidase solution (50 units ml⁻¹). The amount of DNA was quantified by PicoGreen dsDNA reagent according to the manufacturer's protocol. Briefly, the cell pellets were lysed by a freeze–thaw cycle in 200 µl of DNA-free lysis buffer. Samples were then incubated with 200 µl of PicoGreen working solution. The number of cells attached to the surface was then determined by the fluorescence measurement of the sample solution along with the known concentration of cell suspension for the standard curve. The fluorescence measurement was performed in four replicates using a microplate reader with excitation and emission at 480 and 520 nm, respectively.

The assessment of HUVEC cell adhesion was performed 2 days after the cells were seeded. Prior to immunostaining using an Actin focal adhesion stain kit, the cells on the surfaces of the hydrogels were fixed with 4% formaldehyde solution at room temperature for 20 min. After washing, the cells were permeabilized using 0.5% Triton X-100 in PBS solution at room temperature for 5 min. The cells were then blocked in 0.05% Triton X-100 containing 1% bovine serum albumin at room temperature for 1 h. The samples were then incubated with anti-vinculin in blocking buffer solution at 4 °C overnight. After washing, the cells were incubated with the fluorescein isothiocyanate (FITC)-conjugated secondary antibody in the dark for 30 min. For double labeling, TRITC-conjugated phalloidin was incubated simultaneously with the secondary antibody. The cell nuclei were counterstained with DAPI (1:15,000 in water of 5 mg ml⁻¹ stock). Confocal images were taken with a confocal laser scanning microscope (Olympus FV300, Japan). For each sample, the cells in five regions on the surface were randomly selected from the images. The size of the cells were estimated by Image-Pro-Plus software and averaged to give the cell spread-out area.

2.7. In vitro 3-D culture in hydrogel

For 3-D cell culture in HA–Tyr–RGD hydrogels, HFF-1 and HUVECs (1:1) were mixed with HA–Tyr solution (1 wt.%) and phenol₂–PEG–RGD (0.1 or 0.2 mM) at a final total cell density of 4×10^6 cells ml⁻¹ in 250 µl. The initiation of gel formation was performed using HRP and H₂O₂ as described above. The hydrogels containing cells were allowed to set for 4 h before being maintained in culture medium. HA–Tyr hydrogel without the addition of phenol₂–PEG–RGD was prepared using the same protocol to serve as a comparison. The culture medium was exchanged every 2–3 days. The cell number was determined by DNA quantification assay as described above. To quantify the length of vessel network formed by HUVECs, the cell-laden hydrogel was fixed and the similar immunostaining protocol was followed as described above. The capillary-like network of HUVECs was visualized by FITC-conjugated secondary antibody against CD31 antibody after the immunostaining process was completed. The average length of the capillary-like network was then examined on randomly selected cells on 3-D projected confocal images.

To access outward migration of HUVECs from the various hydrogels, cells were pre-labeled with CellTracker Green CMFDA at 25 µM for 30 min and encapsulated in the hydrogels with or without phenol₂–PEG–RGD. The gels were formed as described previously on the apical side of the FuoroBlok inserts. EGM-2 medium with fresh vascular endothelial growth factor (VEGF) and fibroblast growth factor (FGF) (2 ng ml⁻¹, according to the manufacturer) was added to lower chamber and replaced every 24 h to act as chemoattractants. EGM-2 medium without growth factors was added to the inserts on top of the cell-laden hydrogels. At predetermined time intervals, fluorescence intensity from the basal side was measured in bottom-reading mode using a microplate

reader with excitation and emission at 492 and 517 nm, respectively. The fluorescence intensity relative to 0 h for each sample was recorded. The experiments were performed in four replicates. The morphology of fluorescently labeled cells was accessed using a fluorescence microscope (Olympus 71, Japan).

2.8. Formation of functional human vasculature by injectable hydrogel system

Nonobese diabetic/severe combined immunodeficiency (NOD/SCID) mice that were supplied by Biological Resource Center (BRC) in Biopolis, Singapore were used at 6–8 weeks of age. The cell-laden hydrogel was prepared in a similar way as described earlier with slight modification. Briefly, HUVECs and HFF1 (1:1) were embedded in 250 μl of HA-Tyr or HA-Tyr-RGD hydrogel precursor solution at a final total cell density of 4×10^6 cells ml^{-1} . Prior to injection, a predetermined amount of HRP and H_2O_2 was added to the precursor solution. 100 μl of the solution was then injected subcutaneously through a 22-gauge needle into the backs of mice. On day 14 after the injection, 100 μl of rhodamine-dextran solution (1.5 wt.%) was injected into the mice via the tail vein, to illuminate newly formed vasculature in the hydrogel construct before it was harvested and viewed under a fluorescence microscope. The samples for histological analysis were fixed with 4% paraformaldehyde for 24 h at 4 °C and immersed in 30% sucrose solution overnight before being embedded in OCT cryostat embedding medium (Tissue-Tek[®], Sakura Finetek, USA). Cryostat sections were then cut and collected on silane-coated slides. The slides were stained with hematoxylin and eosin (H&E) and immunohisto-stained with human nuclei antibody. Chromogenic detection was employed to visualize the stained nuclei in brown using an HRP-DAB staining kit according to the manufacturer's protocol. The care and use of laboratory animals were performed according to the approved protocol of the Institutional Animal Care and Use Committee (IACUC) at the BRC in Biopolis, Singapore.

2.9. Statistical analysis

All data were expressed as mean \pm standard deviation (SD). Differences between the values were assessed using the one-way analysis of variance test using SigmaStat software (Systat Software, Inc.). In this analysis, $p < 0.05$ was considered statistically significant.

3. Results and discussion

3.1. The effect of Ph₂-K on hydrogel formation

Park et al. reported the incorporation of bioactive peptide into a GPT hydrogel via the HRP-mediated coupling reaction [8]. In the study, an endothelial cell binding sequence that terminated with a tyrosine residue (SVVYGLRGGY) was conjugated to the tyramine moieties of GPT. Peptide conjugation resulted in a decrease in the shear storage modulus (G') when the feed concentration of the peptide was increased. The decrease in G' was attributed to the conjugation of peptide into the hydrogel network, resulting in the consumption of tyramine moieties available for the crosslinking reaction. In this study, we designed a peptide bearing two phenol moieties at one extremity which could act as a crosslinker in the hydrogel system.

First, a model molecule composed of a lysine residue flanked by two phenols (Ph₂-K) was synthesized (Fig. S.1) and a systematic study on the effects of Ph₂-K on hydrogel formation, such as G' and gel point, was carried out. 3-(4-Hydroxyphenyl) propionic acid

(HPA), which contains only one phenol moiety, was used as a comparison in the study.

With an addition of HPA, the coupling efficiency of phenol moieties dropped from 85% to 65% as the feed concentration increased from 0.1 to 0.3 mM (Fig. S.2). In contrast, the coupling efficiency remained constant at 85% regardless of the feed concentration of Ph₂-K. The G' of the resultant hydrogel showed a general decline with an addition of either Ph₂-K or HPA (Fig. S.3a). However, the decrease in G' was less pronounced in the case of hydrogels prepared by Ph₂-K, attributed to its di-phenol structure, which could act as a crosslinker. This phenomenon is most likely due to the intrinsic tradeoff between the conjugation of phenol-containing RGD molecules and the crosslinking of the hydrogel network in this one-step modification approach where both processes shared the same reaction mechanism. Moreover, the steric hindrance of the Ph₂-K possibly limited the ability to be fully crosslinked into the hydrogel network, resulting in the decline in G' . It is noteworthy that an increase in the feed concentration of HPA resulted in the increase in gel point from 1.5 to 3.4 min (Fig. S.3b), indicating a decrease in gelation rate. The decrease in gelation rate may not be desirable as rapid gelation is an important requirement for an injectable hydrogel system to prevent the undesirable diffusion of the gel precursors and cells to the surrounding tissues. In a clear contrast, the gelation rate was found to be well maintained in the case of Ph₂-K. Water uptake of hydrogels conjugated with HPA or Ph₂-K was in good agreement with G' of the hydrogel (Fig. S.4). Generally, the hydrogels with the addition of HPA had higher water uptake than the ones with Ph₂-K at the same feed concentration, indicating that the HPA-conjugated hydrogels had lower crosslinking density. Taken together, Ph₂-K demonstrated a more consistent conjugation efficiency, higher G' and faster gelation rate than HPA. Therefore, a bioactive peptide motif bearing two phenol moieties, phenol₂-PEG-RGD, was designed and used to functionalize the HA-Tyr hydrogel system in the following study.

3.2. Synthesis and characterization of phenol₂-PEG-RGD

Phenol₂-PEG-RGD was synthesized with a molecular structure shown in Fig. 1a. Its purity was found to be >98%, as shown in HPLC (Fig. 1b). Electrospray ionization mass spectrometry of the purified product further confirmed the success in the synthesis with peaks at m/z 487.4 for $[\text{M}+2\text{H}]^{2+}$ and 973.5 for $[\text{M}+\text{H}]^+$ (Fig. 1c). The content of phenol moieties in phenol₂-PEG-RGD was analyzed by measuring the absorbance values. HPA, which was used to synthesize phenol₂-PEG-RGD, was employed as a control in this measurement. In the range of wavelengths between 250 and 280 nm, the absorbance value for phenol₂-PEG-RGD was found to be approximately doubled compared to the HPA standard at the same molar concentration. For example, at 276 nm (absorption maxima for phenol moiety), the absorbance for phenol₂-PEG-RGD was 0.381 compared to 0.194 for HPA. This indicated that two HPA molecules were successfully introduced into phenol₂-PEG-RGD by amide formations between amine groups of lysine (K) residue and carboxyl groups of HPA.

3.3. Hydrogel formation and characterization

HA-Tyr-RGD hydrogels consisting of HA-Tyr and phenol₂-PEG-RGD were formed via the enzymatic oxidation coupling of phenol moieties catalyzed by HRP and H_2O_2 (Fig. 2). It has been reported that phenols crosslink through either the more common C–C linkage between the ortho-carbons of the aromatic ring or the C–O linkage between the ortho-carbon and the phenolic oxygen [17]. As a result, RGD peptide motifs were simultaneously conjugated into the hydrogel network during gel formation process. The hydrogels without phenol₂-PEG-RGD, with 0.1 mM and 0.2 mM

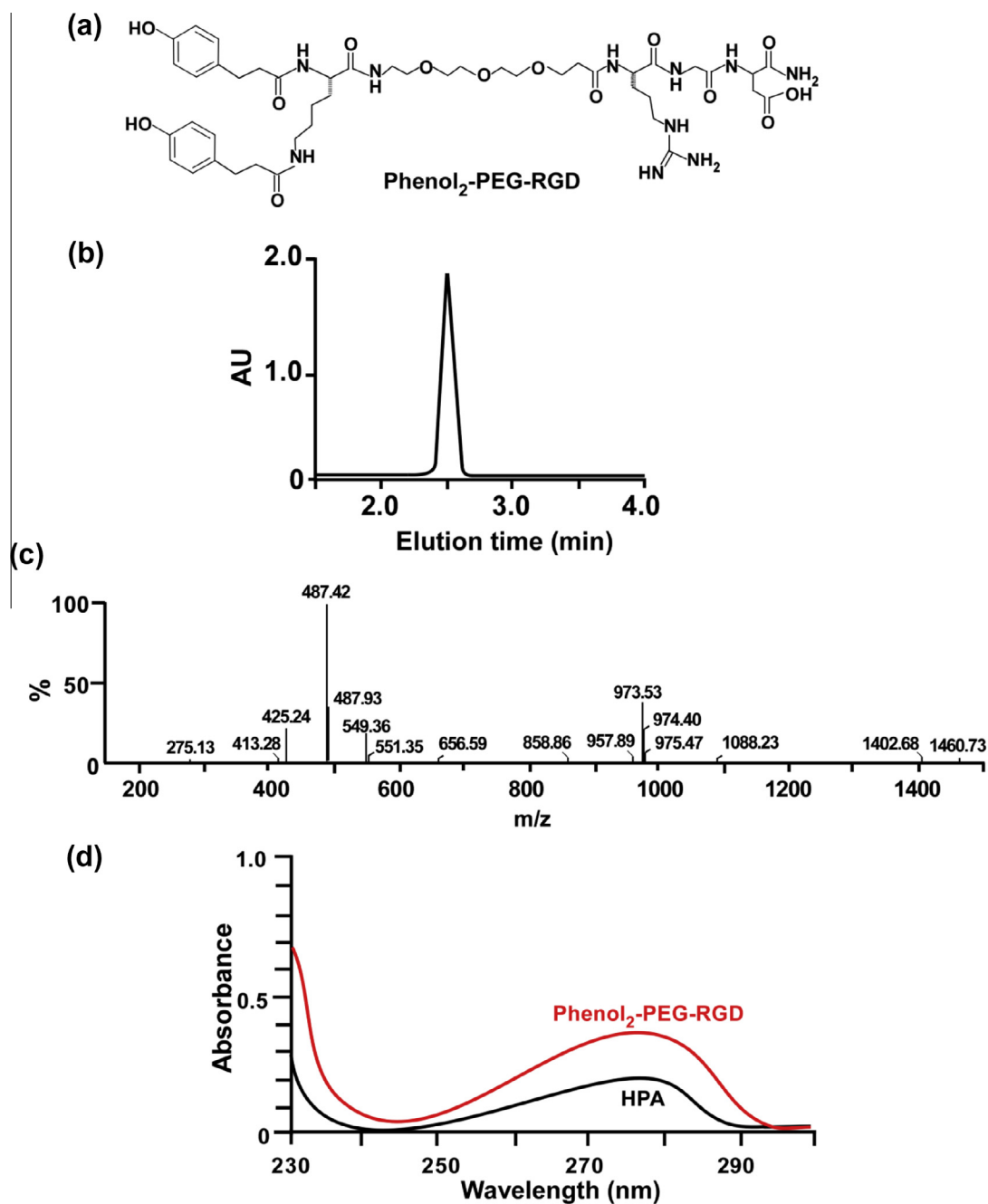


Fig. 1. Synthesis and characterization of phenol₂-PEG-RGD: (a) chemical structure, (b and c) LC-MS analysis and (d) UV-vis spectroscopy of phenol₂-PEG-RGD.

of phenol₂-PEG-RGD are abbreviated as HA-Tyr, HA-Tyr-RGD-0.1 and HA-Tyr-RGD-0.2, respectively.

To determine the coupling efficiency of phenol₂-PEG-RGD after the crosslinking was completed, the amount of unconjugated phenol₂-PEG-RGD leached out from the hydrogel to the PBS solution was quantified by BCA assay after the hydrogel was soaked in PBS solution overnight. As summarized in Table 1, G' of the HA-Tyr was higher than that of RGD-modified HA-Tyr hydrogels when H₂O₂ and HRP concentrations were fixed at 0.43 mM and 0.15 units ml⁻¹, respectively. The conjugation efficiency in the case of HA-Tyr-RGD-0.1 and HA-Tyr-RGD-0.2 was 74% and 71%, respectively. The gel point did not change significantly when the RGD addition was increased from 0.1 to 0.2 mM. It was in good agreement with our observation when the control molecules, Ph₂-K and HPA, were

used and compared. Water uptake of the hydrogels also significantly increased when 0.2 mM of phenol₂-PEG-RGD was used in the modification due to its lower crosslinking density, in agreement with the stiffness measurement (G').

3.4. Effect of the RGD conjugation on HUVEC attachment and proliferation in two dimensions

Prior to performing 3-D cell culture in hydrogels, HUVECs were first seeded on the surface of the hydrogels to evaluate the effect of RGD conjugation in the hydrogel on cell morphology. HA itself has been shown to resist the adhesion of many proteins and cells and is widely used to prevent the formation of postoperative peritoneal adhesions [40]. Fig. 3a shows the confocal fluorescence images of

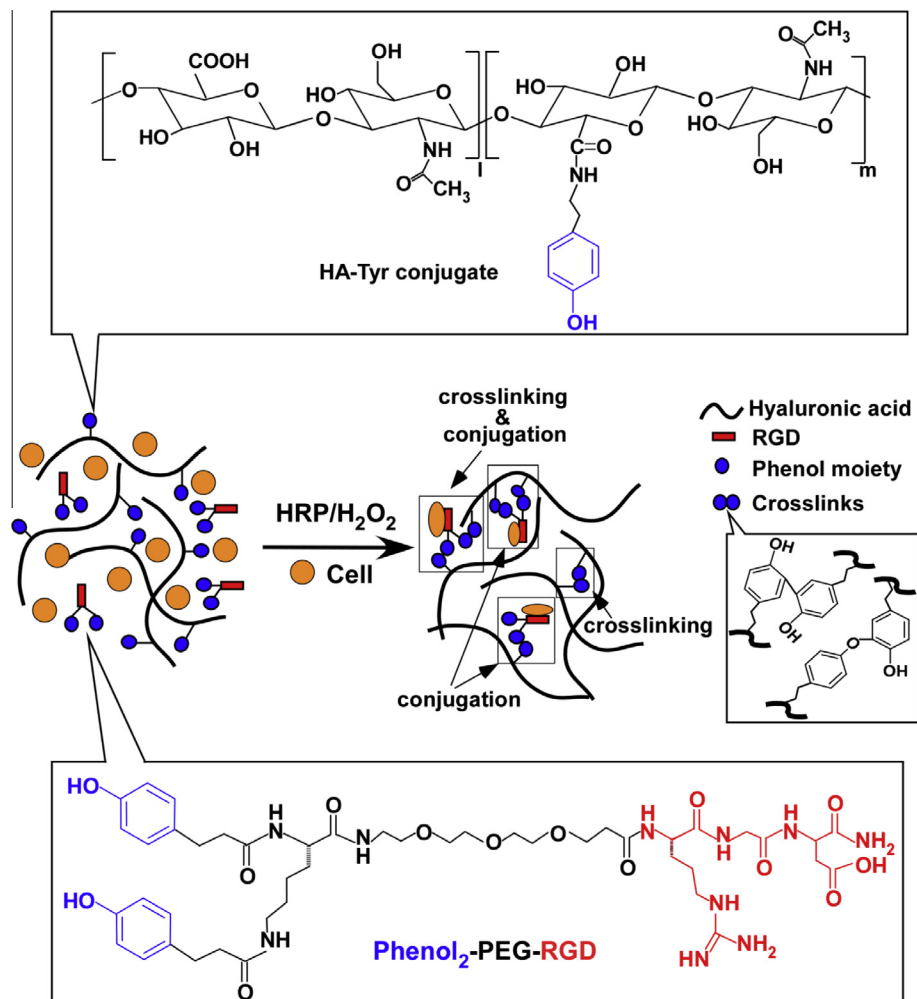


Fig. 2. Enzyme-mediated injectable hydrogel system for the formation of functional human vasculature. Phenol₂-PEG-RGD was conjugated simultaneously into HA-Tyr during in situ gel formation via enzymatic oxidation reaction using HRP and H₂O₂ for 3-D cell culture.

Table 1
Preparation and characterization of HA-Tyr-RGD hydrogels.^a

Hydrogel sample	HA-Tyr conjugate (mg/ml)	Phenol ₂ -PEG-RGD (mM)	Conjugation efficiency of phenol ₂ -PEG-RGD (%)	G' (Pa)	Gel point (min) ^b	Water uptake
HA-Tyr	10	0	–	1215 ± 31	1.6 ± 0.3	51.8 ± 3.4 ^c
HA-Tyr-RGD-0.1	10	0.1	74 ± 4	941 ± 152	1.3 ± 0.2	53.8 ± 0.7 ^c
HA-Tyr-RGD-0.2	10	0.2	71 ± 3	532 ± 36	1.3 ± 0.1	61.4 ± 1.1

^a All hydrogels were prepared using 0.15 units/ml of HRP and 0.43 mM of H₂O₂. Measurement was taken with constant deformation of 1% at 1Hz and 37 °C (n = 4). Results are shown as the average values ± standard deviation.

^b Gel point is defined as the time at which the crossover of storage modulus (G') and loss modulus (G'') occurred. Herein, it is used as an indicator of the rate of gelation.

^c *p* < 0.05 when compared to the value of water uptake calculated for HA-Tyr-RGD-0.2

focal adhesion and actin cytoskeleton in HUVECs. These images revealed focal contacts in green using an anti-vinculin monoclonal antibody, F-actin in red and cell nuclei in blue. The cells on the surface of unmodified HA-Tyr hydrogel were found to be round. In contrast, the cells appeared to adhere strongly onto the HA-Tyr-RGD hydrogel surface with spread-out morphology. Both the focal contact and F-actin organization were found to be diffused. This was in good agreement with our earlier reports on cell responses to the hydrogels of comparable storage modulus (G'). Both focal contact and F-actin showed a progressive trend from being

diffused when in contact with soft hydrogels (G' = 0.6–2.5 kPa) to having more structure arrangements when cells were attached to the stiffer ones (G' = 8.1 kPa) [39].

The cell spread-out area was further quantified using ImagePro-Plus software. The HUVECs on the RGD-modified HA-Tyr had at least a fourfold increase in cell spreading area (Fig. 3b) and was found to be significantly different compared to the unmodified HA-Tyr (*p* < 0.01). The results indicated that the conjugation of RGD significantly altered the cell attachment behavior and largely improved the HUVEC adhesion. Moreover, cell adhesion was strong

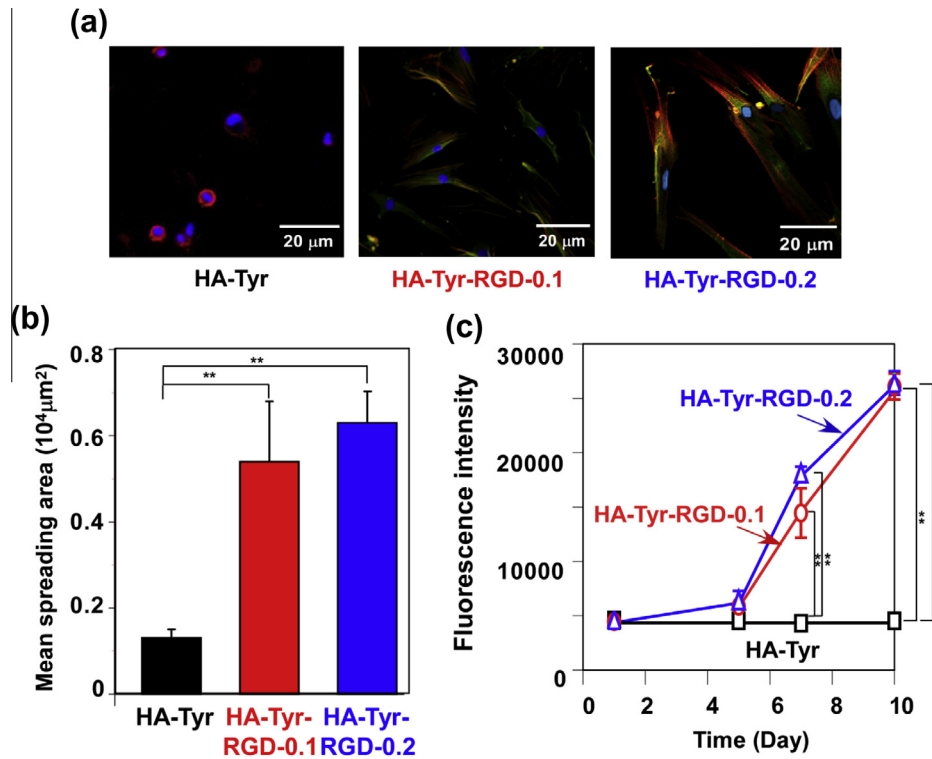


Fig. 3. (a) Confocal fluorescence microscopy of focal adhesion and actin cytoskeleton in HUVECs cultured on the hydrogels with vinculin, F-actin, nuclei shown in green, red and blue, respectively. (b) HUVEC spreading on the surface of HA-Tyr and HA-Tyr-RGD hydrogels after 24 h incubation. (c) 2-D HUVEC proliferation on the hydrogels. The hydrogels with phenol₂-PEG-RGD (0.1 mM or 0.2 mM) are abbreviated respectively, HA-Tyr-RGD-0.1 and HA-Tyr-RGD-0.2. Results are shown as the average values \pm standard deviation. ** $p < 0.01$ between groups ($n = 4$).

and stable enough to induce steady cell growth over time, as shown in Fig. 3c, in clear contrast to the non-proliferative cells on the unmodified HA-Tyr hydrogels. Interestingly, no statistically significant increase in cell spreading and proliferation was observed when the phenol₂-PEG-RGD concentration was further increased from 0.1 mM to 0.2 mM. This increase in the concentration of phenol₂-PEG-RGD resulted in the HA-Tyr-RGD-0.2 of lower stiffness compared to HA-Tyr-RGD-0.1. As reported previously, the cell proliferation was often directly correlated to the stiffness of the substrate where cells resided in the 2-D cell culture study [39]. The result suggested that failing to observe the effect of the further increase in RGD concentration on proliferation rate in HA-Tyr-RGD-0.2 could be attributed to its lower stiffness (G').

3.5. Effect of RGD conjugation on HUVEC migration and proliferation in 3-D

The cytotoxicity potency of H₂O₂ in the presence of HRP was investigated prior to this 3-D culture study. It was found that in the presence of HRP, H₂O₂ participated predominantly in the enzymatic oxidation reaction and exerted minimal toxicity effect on the cell viability when its concentration was up to 0.85 mM. It was in a clear contrast to the high toxicity observed when cells were exposed to H₂O₂ at the same concentrations in the absence of HRP (Fig. S.5). To further assess the potential of using cell-laden HA-Tyr-RGD to stimulate and promote the formation of capillary-like network, HUVECs were incorporated into the precursor solution to form cell-laden hydrogels in situ by HRP and H₂O₂. The migration of HUVECs from HA-Tyr-RGD hydrogels was investigated using a Transwell® system, whereby the HA-Tyr-RGD containing the fluorescence-labeled HUVECs was placed in the apical side of the FluoroBlok® inserts and EGM-2 medium containing fresh VEGF and

FGF was added to the lower chamber (Fig. 4a). A time course of the cell migration through the fluorescence-blocking membrane was monitored for 48 h. The fluorescence intensity, which directly corresponded to the number of cells that migrated through the membrane, was recorded. As shown in Fig. 4b, similar to the findings from the 2-D study, the cells also featured more spread-out morphology inside the HA-Tyr-RGD hydrogel in contrast to the rounded cells inside the HA-Tyr hydrogel. The interaction between the cells and RGD was found to significantly improve not only the cell adhesion but also the cell migration. As shown in Fig. 4c, the number of migratory cells increased over time, differing in rates among the three samples. A significantly higher rate of cell migration was observed when the cells were originally entrapped in hydrogels with RGD modification compared to the HA-Tyr hydrogel without modification at the end of 48 h in this study.

In the proliferation study, the encapsulated HUVECs were able to proliferate within the first week of culture in both HA-Tyr-RGD-0.1 and HA-Tyr-RGD-0.2 hydrogels (Fig. 5). A further increase in RGD addition from 0.1 to 0.2 mM did not seem to enhance the cell proliferation rate significantly in the 3-D culture study, similar to the observation made in the previous 2-D study ($p > 0.05$). Again, the cells in HA-Tyr remained non-proliferative throughout this 3-D study, which was attributed to the inherent cell-repelling nature of HA. Moreover, a sharp decline in cell number was observed in the HA-Tyr-RGD hydrogels when the culture was extended over 1 week regardless of the concentration of the phenol₂-PEG-RGD. This strongly suggested that monoculture of HUVECs could not stabilize its capillary-like network growth in 3-D culture over an extended culture time. This indication was also supported by findings reported previously that fibroblasts and/or fibroblast-derived factors are essential in facilitating endothelial morphogenesis into capillary-like tubes and improving stability

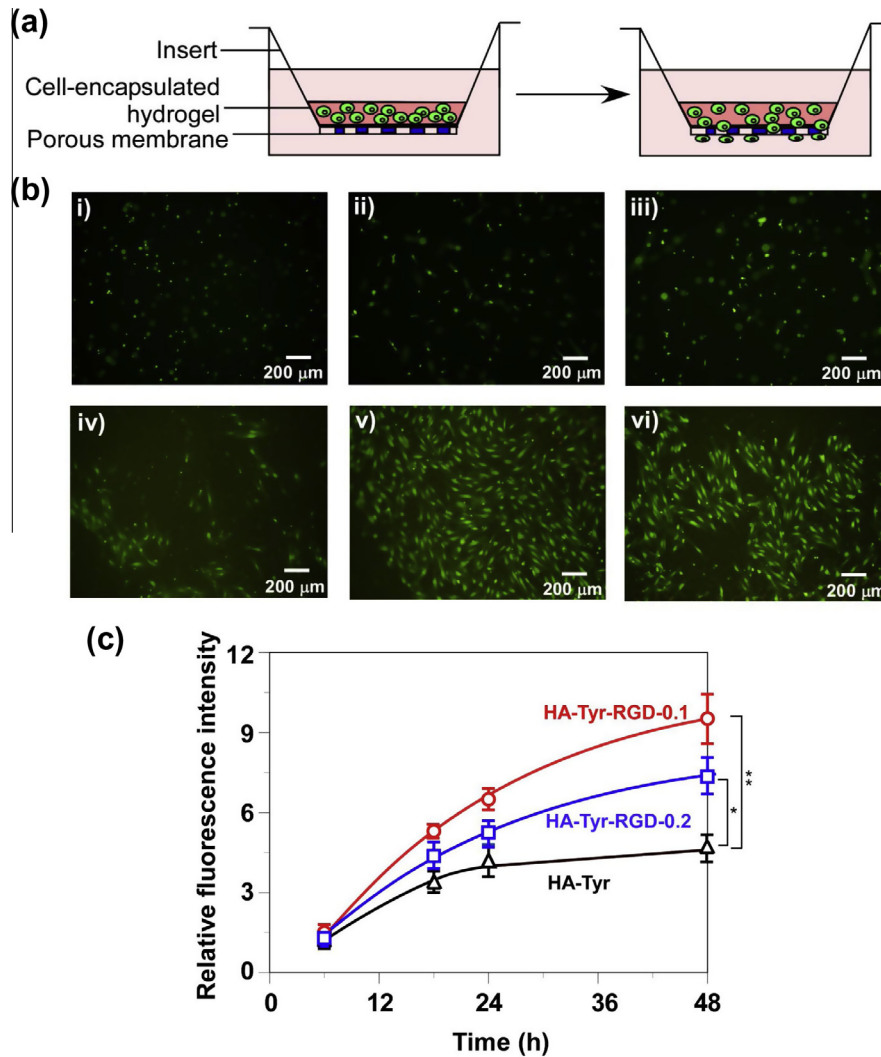


Fig. 4. Migration of HUVECs in hydrogels. (a) Schematic illustration of migration study in vitro. (b) Representative fluorescence images of CellTracker™-labelled cells that remained in (i) HA-Tyr, (ii) HA-Tyr-RGD-0.1 and (iii) HA-Tyr-RGD-0.2 hydrogels and had migrated through FluoroBlok membrane from (iv) HA-Tyr, (v) HA-Tyr-RGD-0.1 and (vi) HA-Tyr-RGD-0.2 hydrogels at 24 h. (c) Fluorescence intensity (relative to 0 h) of fluorescently labeled HUVECs that migrated through FluoroBlok membrane over time. Results are shown as the average values \pm standard deviation. * $p < 0.05$ and ** $p < 0.01$ between groups ($n = 4$).

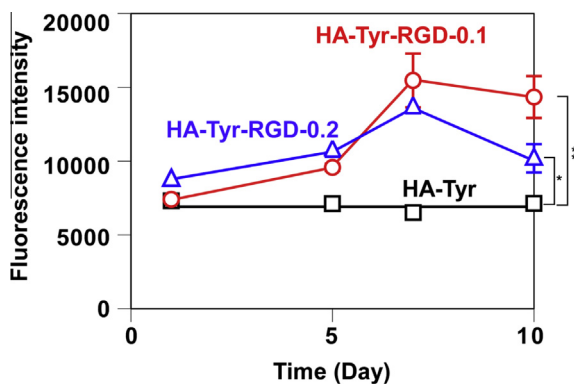


Fig. 5. 3-D HUVEC proliferation in HA-Tyr and HA-Tyr-RGD hydrogels. Results are shown as the average values \pm standard deviation. * $p < 0.05$ and ** $p < 0.01$ between groups ($n = 6$).

of newly formed capillary sprouts for induction of angiogenesis [28,41].

Based on the results, we sought to study the effects of 3-D co-culture of HUVECs with human fibroblasts (HFF1) on the formation

of capillary-like network and stabilization of such a network using the HA-Tyr-RGD-0.1 as a model hydrogel. The HA-Tyr hydrogel was used as a control. As shown in Fig. 6a, the cell morphology in the HA-Tyr hydrogel showed only a round shape. In contrast, the HA-Tyr hydrogel with RGD modification strongly supported the spreading of the encapsulated cells within the 3-D hydrogel matrix and the formation of cell-cell contacts with capillary-like structures. As shown as the inset in Fig. 6a(iii), these capillary-like structures with branches were observed when the HUVECs were co-cultured with HFF1. To ascertain that the capillary-like network measured only comprised endothelial cells, the anti-CD31 antibody known to label HUVECs was used. Fig. 6a(iv) shows the capillary-like network formed by CD31 positive HUVECs.

Next, we examined the effects of culture modes including monoculture and 3-D culture of HUVECs with human fibroblasts (HFF1) on the surfaces of the hydrogels (2-D HFF1/3-D HUVEC) and mixed co-culture on HUVEC capillary-like network formation (Fig. 6b). The unmodified HA-Tyr did not support the formation of the capillary-like network in three dimensions regardless of the culture modes due to the inherent cell-repelling characteristics of HA. The length of the capillary-like network formed by the HUVECs continued to increase in the two co-culture modes over time in the HA-Tyr-RGD hydrogel, but not in the monoculture

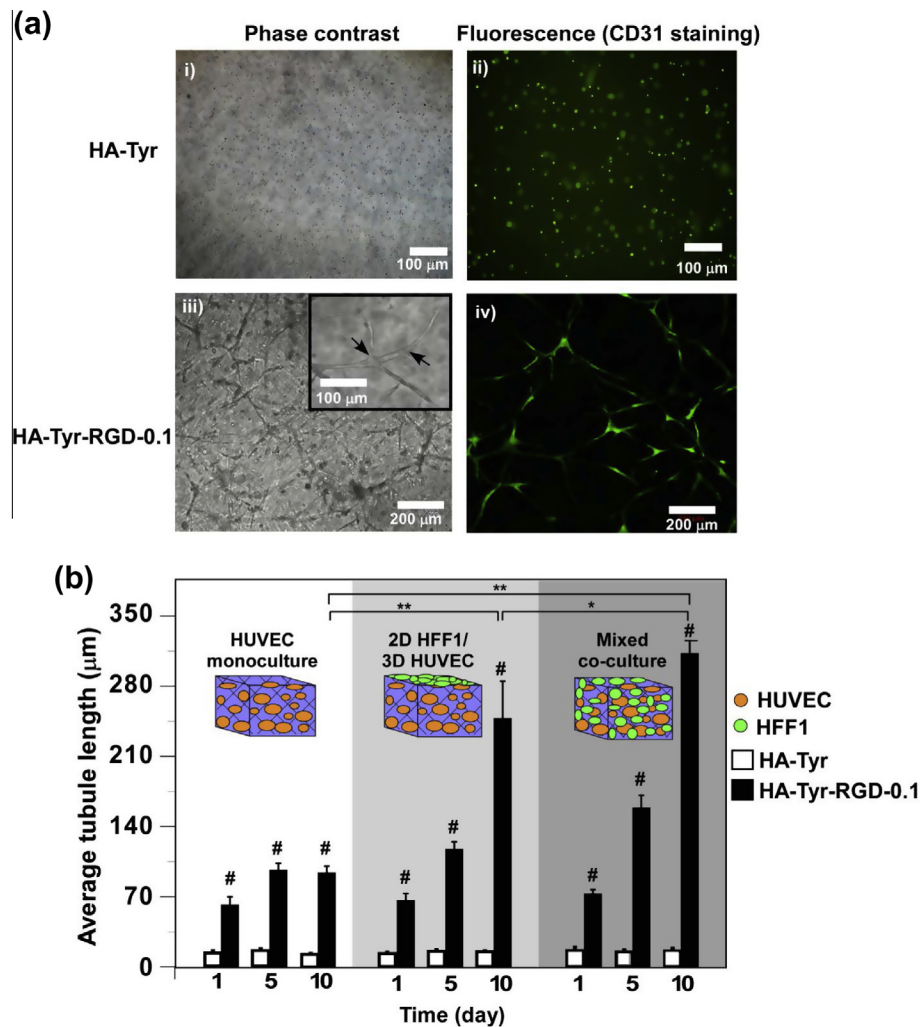


Fig. 6. (a) Representative microscopic and fluorescence images of mixed co-culture of HFF1 and HUVECs in (i and ii) HA-Tyr and (iii and iv) HA-Tyr-RGD-0.1 hydrogels, respectively. Capillary-like structure with branches (black arrows) was found in HA-Tyr-RGD-0.1 hydrogels (inset in iii). Fluorescence images were acquired by staining of HUVECs with CD31 antibody. (b) Length of HUVEC capillary-like tube formed inside HA-Tyr and HA-Tyr-RGD hydrogels in three different culture modes, namely monoculture of HUVEC, 2-D HFF1/3-D HUVECs and mixed co-culture of HFF1 and HUVEC. Results are shown as the average values \pm standard deviation. * $p < 0.05$ and ** $p < 0.01$ between groups, # $p < 0.01$ when compared to the HA-Tyr group at the same experimental condition ($n = 6$).

mode when the culture time was over 5 days. The cells in the co-culture modes with HFF1 showed significantly greater value in average tubule length at the end of 10 days of culture compared to that in the monoculture condition ($p < 0.01$). In addition, the average tubule length of the HUVECs inside the RGD-modified HA-Tyr hydrogels was significantly higher than that of the cells in the unmodified one at any given experimental condition in this study. Moreover, between the two co-culture modes, the mixed co-culture mode was found to be superior to 2-D HFF1/3-D HUVECs with a significantly greater in average length of the vessel network ($p < 0.05$) at the end of 10 days of culture. This was likely due to a closer proximity between the cells, hence better diffusion of fibroblast-mediated factors and cellular crosstalk to facilitate endothelial morphogenesis into capillary-like tubes in mixed co-culture mode. This finding is also supported by a previous report on the improvement of capillary morphogenesis by distributing fibroblasts throughout the matrix to overcome the diffusion restriction [42].

3.6. In vivo vascularization by injectable HA-Tyr-RGD hydrogel system

To evaluate the effects of RGD modification and co-culture of HUVECs and HFF1 on vascularization potential of the cell-laden

hydrogels in vivo, HA-Tyr-RGD-0.1 with embedded HUVECs or a mixture of HUVECs and HFF1 (1:1) was selected for this study. Unmodified HA-Tyr hydrogel was used as a comparison. Briefly, hydrogel precursor solutions with the HUVECs alone or the mixture of HUVECs and HFF1 were injected to the back of mice, and the cell-laden hydrogels were formed in situ (Fig. 7a). On day 14 after the injection, tail-vein injection of rhodamine-dextran was performed to illuminate newly formed vasculature in the hydrogel construct under fluorescence microscopy.

Newly formed vasculature in the implanted hydrogel construct was observed visually in both HA-Tyr-RGD-0.1 with HUVECs and HA-Tyr-RGD-0.1 with both HUVECs and HFF1 (Fig. 7b), but not in unmodified HA-Tyr with the two cell types. This suggests that RGD conjugation in the hydrogel system played an important role in stimulating the endothelial cell activity. Furthermore, there were more newly formed vessels in the HA-Tyr-RGD-0.1 with both HUVECs and HFF1, underlining the importance of cellular crosstalk between HUVECs and HFF1 for vascular formation. Direct observation of the vasculature formation in the freshly harvested hydrogel construct illuminated by rhodamine-dextran solution under fluorescence microscopy was performed. The fluorescence images are shown in Fig. 7c. It became evident that the vasculature had anastomosed with the host, and the rhodamine-dextran solution was

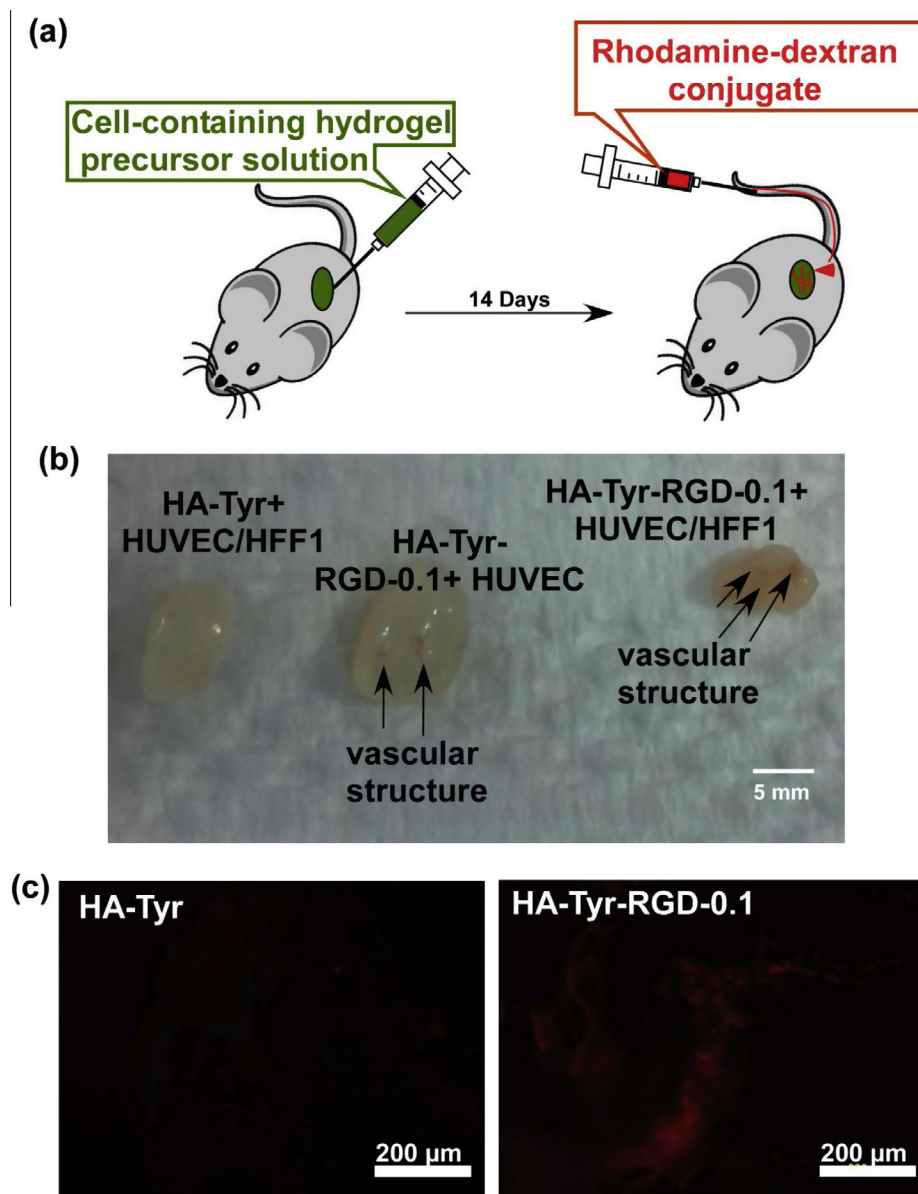


Fig. 7. In vivo evaluation of the formation of functional human vasculature using cell-laden HA-Tyr-RGD hydrogels. HA-Tyr-RGD hydrogel precursor solution consisting of 10 mg ml^{-1} HA-Tyr, $0.15 \text{ units ml}^{-1}$ of HRP, 0.43 mM of H_2O_2 , 0.1 mM of phenol₂-PEG-RGD and cells at total density of $4 \times 10^6 \text{ cells ml}^{-1}$ was injected subcutaneously through a 21-gauge needle into the backs of mice. HA-Tyr hydrogel containing both HUVECs and HFF1 at the same cell density was served as comparison. (a) Schematic graph of in vivo evaluation. (b) Photographic views of harvested gels with vasculature formed after 14 days. (c) Direct observation of the vasculature formation in the freshly harvested hydrogel constructs illuminated by tail vein injection of rhodamine-dextran solution. (d) H&E fluorescence images illuminated by the presence of rhodamine-dextran and immunostain of human nuclei on sections from the HA-Tyr and HA-Tyr-RGD-0.1 hydrogels with incorporation of both HUVECs and HFF1 on day 14.

able to reach and diffuse into this newly formed vasculature inside the HA-Tyr hydrogel with RGD modification but not in the unmodified HA-Tyr hydrogel.

Hematoxylin and eosin (H&E) staining and immunohistochemistry analysis on human nuclei were employed to further confirm the vasculature formation, as well as whether the newly formed vasculature comprised cells of human origin. As revealed in Fig. 7d, there was no visible capillary formation on the sections from HA-Tyr without RGD modification. However, on the sections from cell-laden HA-Tyr-RGD-0.1 with the HUVEC (Fig. S.6) or the mixture of HUVECs and HFF1 (Fig. 7c), visible vasculatures were observed, which co-localized well with their corresponding fluorescence images. Furthermore, immunohistochemistry analysis confirmed that the vasculature consisted of cells which stained positive for human nuclei antibody. Taken together, it was evident that HA-Tyr-RGD-0.1 hydrogel with co-culture of HUVEC/HFF1

was able to support HUVEC activity inside the hydrogel and enhance its bioactivities, leading to promotion of vascularization in the hydrogel construct. In addition, this newly improved hydrogel system consisting of HA-Tyr and RGD peptide motif provides a simple and effective means to design injectable hydrogels with additional bioactive agents for enhanced vascularization. We believe that this in situ enzymatic incorporation approach could be applied to other single or multiple bioactive motifs, not limited to RGD, for specific functions of cells of interest for tissue engineering and regeneration.

4. Conclusions

One-step preparation of a multi-functional injectable HA-based hydrogel system was successfully developed. A phenol₂-PEG-RGD

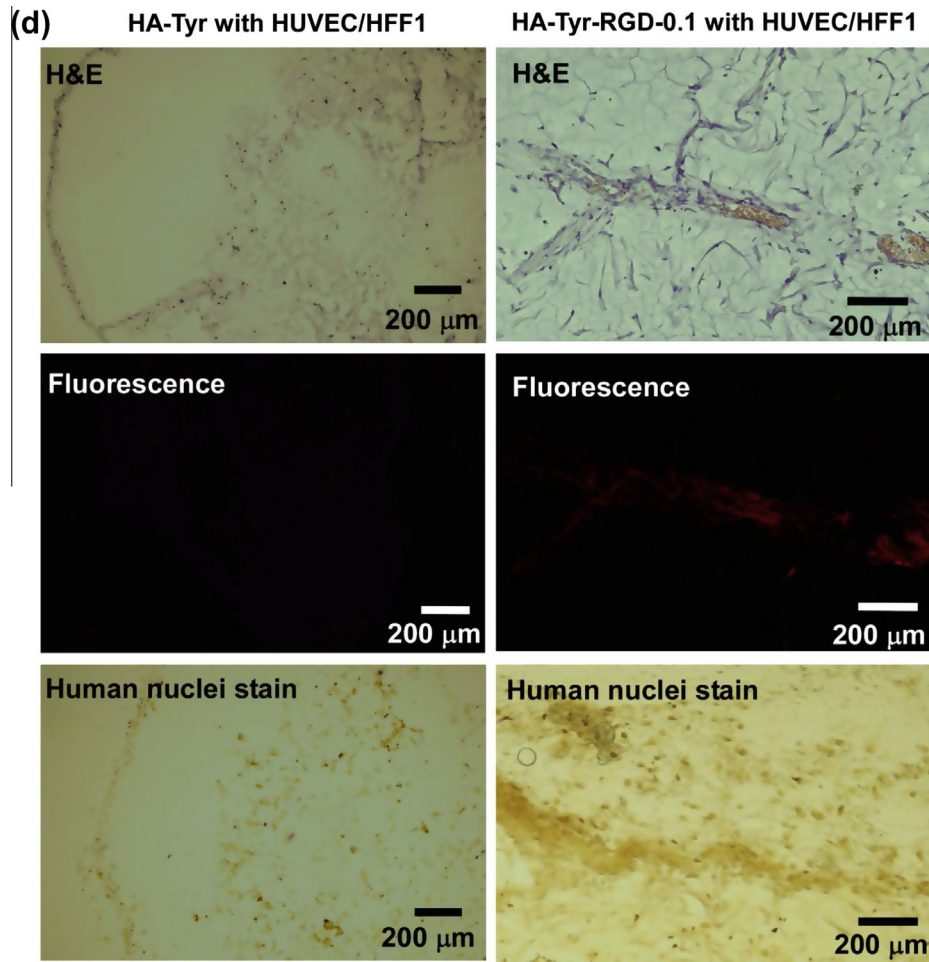


Fig. 7 (continued)

molecule containing two phenol moieties per molecule at one extremity was found to be efficient in retaining conjugation efficiency to the hydrogel matrix. The HA-Tyr hydrogel modified with phenol₂-PEG-RGD demonstrated a significant improvement in facilitating HUVEC adhesion, proliferation and migration, as well as capillary-like network formation and extension, in combination with co-culture of HUVECs and HFF1 in vitro compared to an unmodified counterpart. In vivo formation of vasculature in the cell-laden hydrogel constructs illuminated by rhodamine-dextran via tail-vein confirmed the anastomosis with the host vasculature. In combination with the inherent properties of HA that favor angiogenesis and RGD peptide motifs promoting cell adhesion, the HA-Tyr-RGD hydrogel demonstrated its active role in promoting the formation of vasculature. This simple and effective means to integrate bioactive molecules during hydrogel formation via enzymatic oxidation reaction by HRP and H₂O₂ provides a platform for engineering multi-functional injectable hydrogels with additional bioactivities that are not naturally present for various biomedical applications.

Acknowledgements

This work was supported by the Institute of Bioengineering and Nanotechnology (Biomedical Research Council, Agency for Science, Technology and Research, Singapore). We thank JNC Corp., Japan, for the generous gift of hyaluronic acid.

Appendix A. Figures with essential colour discrimination

Certain figures in this article, particularly Figs. 1–7 are difficult to interpret in black and white. The full colour images can be found in the on-line version, at <http://dx.doi.org/10.1016/j.actbio.2014.02.022>.

Appendix B. Supplementary data

Supplementary data associated with this article can be found, in the online version, at <http://dx.doi.org/10.1016/j.actbio.2014.02.022>.

References

- [1] Alsberg E, Anderson KW, Albeiruti A, Rowley JA, Mooney DJ. Engineering growing tissues. *Proc Natl Acad Sci USA* 2002;99:12025–30.
- [2] Bidarra SJ, Barrias CC, Fonseca KB, Barbosa MA, Soares RA, Granja PL. Injectable in situ crosslinkable RGD-modified alginate matrix for endothelial cells delivery. *Biomaterials* 2011;32:7897–904.
- [3] Oliviero O, Ventre M, Netti PA. Functional porous hydrogels to study angiogenesis under the effect of controlled release of vascular endothelial growth factor. *Acta Biomater* 2012;8:3294–301.
- [4] Park YD, Tirelli N, Hubbell JA. Photopolymerized hyaluronic acid-based hydrogels and interpenetrating networks. *Biomaterials* 2003;24:893–900.
- [5] Kraehenbuehl TP, Zammaretti P, Van der Vlies AJ, Schoenmakers RG, Lutolf MP, Jaconi ME, et al. Three-dimensional extracellular matrix-directed cardioprogenitor differentiation: systematic modulation of a synthetic cell-responsive PEG-hydrogel. *Biomaterials* 2008;29:2757–66.

- [6] Lutolf MP, Hubbell JA. Synthetic biomaterials as instructive extracellular microenvironments for morphogenesis in tissue engineering. *Nat Biotechnol* 2005;23:47–55.
- [7] Lutolf MP, Raeber GP, Zisch AH, Tirelli N, Hubbell JA. Cell-responsive synthetic hydrogels. *Adv Mater* 2003;15:888–91.
- [8] Park KM, Lee Y, Son JY, Bae JW, Park KD. In situ SVVYGLR peptide conjugation into injectable gelatin-poly(ethylene glycol)-tyramine hydrogel via enzyme-mediated reaction for enhancement of endothelial cell activity and neovascularization. *Bioconjugate Chem* 2012;23:2042–50.
- [9] Shu XZ, Ghosh K, Liu YC, Palumbo FS, Luo Y, Clark RA, et al. Attachment and spreading of fibroblasts on an RGD peptide-modified injectable hyaluronan hydrogel. *J Biomed Mater Res A* 2004;68A:365–75.
- [10] Schense JC, Bloch J, Aebischer P, Hubbell JA. Enzymatic incorporation of bioactive peptides into fibrin matrices enhances neurite extension. *Nat Biotechnol* 2000;18:415–9.
- [11] Bae KH, Wang L-S, Kurisawa M. Injectable biodegradable hydrogels: progress and challenges. *J Mater Chem B* 2013;1:5371–88.
- [12] Ibrahim S, Ramamurthi A. Hyaluronic acid cues for functional endothelialization of vascular constructs. *J Tissue Eng Regen Med* 2008;2:22–32.
- [13] Yee D, Hanjaya-Putra D, Bose V, Luong E, Gerech S. Hyaluronic acid hydrogels support cord-like structures from endothelial colony-forming cells. *Tissue Eng A* 2011;17:1351–61.
- [14] Lei YG, Gogjini S, Lam J, Segura T. The spreading, migration and proliferation of mouse mesenchymal stem cells cultured inside hyaluronic acid hydrogels. *Biomaterials* 2011;32:39–47.
- [15] Seidlits SK, Drinnan CT, Petersen RR, Shear JB, Suggs LJ, Schmidt CE. Fibronectin-hyaluronic acid composite hydrogels for three-dimensional endothelial cell culture. *Acta Biomater* 2011;7:2401–9.
- [16] Suri S, Schmidt CE. Photopatterned collagen-hyaluronic acid interpenetrating polymer network hydrogels. *Acta Biomater* 2009;5:2385–97.
- [17] Lee F, Kurisawa M. Formation and stability of interpenetrating polymer network hydrogels consisting of fibrin and hyaluronic acid for tissue engineering. *Acta Biomater* 2013;9:5143–52.
- [18] Chen YC, Lin RZ, Qi H, Yang YZ, Bae HJ, Melero-Martin JM, et al. Functional human vascular network generated in photocrosslinkable gelatin methacrylate hydrogels. *Adv Funct Mater* 2012;22:2027–39.
- [19] Cuchiara MP, Gould DJ, McHale MK, Dickinson ME, West JL. Integration of self-assembled microvascular networks with microfabricated PEG-based hydrogels. *Adv Funct Mater* 2012;22:4511–8.
- [20] Lutolf MP, Hubbell JA. Synthesis and physicochemical characterization of end-linked poly(ethylene glycol)-co-peptide hydrogels formed by Michael-type addition. *Biomacromolecules* 2003;4:713–22.
- [21] Lutolf MP, Lauer-Fields JL, Schmoekel HG, Metters AT, Weber FE, Fields GB, et al. Synthetic matrix metalloproteinase-sensitive hydrogels for the conduction of tissue regeneration: engineering cell-invasion characteristics. *Proc Natl Acad Sci USA* 2003;100:5413–8.
- [22] Allen P, Melero-Martin J, Type Bischoff J. Collagen, fibrin and PuraMatrix matrices provide permissive environments for human endothelial and mesenchymal progenitor cells to form neovascular networks. *J Tissue Eng Regen Med* 2011;5:E74–86.
- [23] Hao XJ, Silva EA, Mansson-Broberg A, Grinnemo KH, Siddiqui AJ, Dellgren G, et al. Angiogenic effects of sequential release of VEGF-A(165) and PDGF-BB with alginate hydrogels after myocardial infarction. *Cardiovasc Res* 2007;75:178–85.
- [24] Lee WY, Wei HJ, Wang JJ, Lin KJ, Lin WW, Chen DY, et al. Vascularization and restoration of heart function in rat myocardial infarction using transplantation of human cbMSC/HUVEC core-shell bodies. *Biomaterials* 2012;33:2127–36.
- [25] Leslie-Barbick JE, Saik JE, Gould DJ, Dickinson ME, West JL. The promotion of microvasculature formation in poly(ethylene glycol) diacrylate hydrogels by an immobilized VEGF-mimetic peptide. *Biomaterials* 2011;32:5782–9.
- [26] Moon JJ, West JL. Vascularization of engineered tissues: approaches to promote angiogenesis in biomaterials. *Curr Top Med Chem* 2008;8:300–10.
- [27] Phelps EA, Landazuri N, Thule PM, Taylor WR, Garcia AJ. Bioartificial matrices for therapeutic vascularization. *Proc Natl Acad Sci USA* 2010;107:3323–8.
- [28] Sukmana I, Vermette P. The effects of co-culture with fibroblasts and angiogenic growth factors on microvascular maturation and multi-cellular lumen formation in HUVEC-oriented polymer fibre constructs. *Biomaterials* 2010;31:5091–9.
- [29] Takayama T, Taguchi T, Koyama H, Sakari M, Kamimura W, Takato T, et al. The growth of a vascular network inside a collagen-citric acid derivative hydrogel in rats. *Biomaterials* 2009;30:3580–7.
- [30] Zorlutuna P, Annabi N, Camci-Unal G, Nikkha M, Cha JM, Nichol JW, et al. Microfabricated biomaterials for engineering 3D tissues. *Adv Mater* 2012;24:1782–804.
- [31] Kurisawa M, Chung JE, Yang YY, Gao SJ, Uyama H. Injectable biodegradable hydrogels composed of hyaluronic acid-tyramine conjugates for drug delivery and tissue engineering. *Chem Commun* 2005:4312–4.
- [32] Lee F, Chung JE, Kurisawa M. An injectable enzymatically crosslinked hyaluronic acid-tyramine hydrogel system with independent tuning of mechanical strength and gelation rate. *Soft Matter* 2008;4:880–7.
- [33] Pek YS, Kurisawa M, Gao S, Chung JE, Ying JY. The development of a nanocrystalline apatite reinforced crosslinked hyaluronic acid-tyramine composite as an injectable bone cement. *Biomaterials* 2009;30:822–8.
- [34] Wang HB, Liu ZQ, Li DX, Guo X, Kasper FK, Duan CM, et al. Injectable biodegradable hydrogels for embryonic stem cell transplantation: improved cardiac remodelling and function of myocardial infarction. *J Cell Mol Med* 2012;16:1310–20.
- [35] Xu KM, Lee F, Gao SJ, Chung JE, Yano H, Kurisawa M. Injectable hyaluronic acid-tyramine hydrogels incorporating interferon-alpha 2a for liver cancer therapy. *J Controlled Release* 2013;166:203–10.
- [36] Jin R, Hiemstra C, Zhong ZY, Feijen J. Enzyme-mediated fast in situ formation of hydrogels from dextran-tyramine conjugates. *Biomaterials* 2007;28:2791–800.
- [37] Lee F, Chung JE, Kurisawa M. An injectable hyaluronic acid-tyramine hydrogel system for protein delivery. *J Controlled Release* 2009;134:186–93.
- [38] Kurisawa M, Lee F, Wang LS, Chung JE. Injectable enzymatically crosslinked hydrogel system with independent tuning of mechanical strength and gelation rate for drug delivery and tissue engineering. *J Mater Chem* 2010;20:5371–5.
- [39] Wang LS, Boulaire J, Chan PP, Chung JE, Kurisawa M. The role of stiffness of gelatin-hydroxyphenylpropionic acid hydrogels formed by enzyme-mediated crosslinking on the differentiation of human mesenchymal stem cell. *Biomaterials* 2010;33:8608–16.
- [40] Khademhosseini A, Suh KY, Yang JM, Eng G, Yeh J, Levenberg S, et al. Layer-by-layer deposition of hyaluronic acid and poly-L-lysine for patterned cell co-cultures. *Biomaterials* 2004;25:3583–92.
- [41] Eckermann CW, Lehle K, Schmid SA, Wheatley DN, Kunz-Schughart LA. Characterization and modulation of fibroblast/endothelial cell co-cultures for the in vitro preformation of three-dimensional tubular networks. *Cell Biol Int* 2011;35:1097–110.
- [42] Ghajar CM, Chen X, Harris JW, Suresh V, Hughes CCW, Jeon NL, et al. The effect of matrix density on the regulation of 3-D capillary morphogenesis. *Biophys J* 2008;94:1930–41.